Cellular metabolism regulates contact sites between vacuoles and mitochondria

Hönscher, Carina; Mari, Muriel; Auffarth, Kathrin; Bohnert, Maria; Griffith, Janice; Geerts, Willie; van der Laan, Martin; Cabrera, Margarita; Reggiori, Fulvio; Ungermann, Christian

Published in:
Developmental Cell

DOI:
10.1016/j.devcel.2014.06.006

Publication date:
2014

CellPress

Developmental Cell
Short Article

Cellular Metabolism Regulates Contact Sites between Vacuoles and Mitochondria

Carina Hönscher,[1] Muriel Mari,[2] Kathrin Auffarth,[1] Maria Bohnert,[3] Janice Griffith,[2] Willie Geerts,[4] Martin van der Laan,[3] Margarita Cabrera,[1] Fulvio Reggiori,[2] and Christian Ungermann[1,*]

[1]Biochemistry Section, Department of Biology/Chemistry, University of Osnabrück, Barbarastrasse 13, 49076 Osnabrück, Germany
[2]Department of Cell Biology, Center for Molecular Medicine, University Medical Centre Utrecht, Heidelberglaan 100, 3584 CX Utrecht, the Netherlands
[3]Institute for Biochemistry and Molecular Biology, ZBMZ, and BIOSS Centre for Biological Signalling Studies, University of Freiburg, Stefan-Meier-Strasse 17, 79104 Freiburg, Germany
[4]Molecular Cell Biology, Utrecht University, Padualaan 8, 3584 CH Utrecht, the Netherlands
*Correspondence: cu@uos.de
http://dx.doi.org/10.1016/j.devcel.2014.06.006

SUMMARY

Emerging evidence suggests that contact sites between different organelles form central hubs in the coordination of cellular physiology. Although recent work has emphasized the crucial role of the endoplasmic reticulum in interorganellar crosstalk, the cooperative behavior of other organelles is largely unexplored. Here, we identify a contact site named vCLAMP (*v*acuo*l*e *a*nd *m*itochondria *p*atch) that integrates mitochondria with the lysosome-like vacuole and thus the endocytic pathway. vCLAMPs depend on the vacuolar HOPS tethering complex subunit Vps39/Vam6 and the Rab GTPase Ypt7, which also participate in membrane fusion at the vacuole. Intriguingly, vCLAMPs are located proximal to the ER-mitochondria encounter structure (ERMES) complexes, and an increase in vCLAMPs can rescue the growth defect of ERMES mutants. Importantly, the persistence of vCLAMPs is regulated by phosphorylation of Vps39 and is strongly reduced during respiratory growth. The identification of this organelle contact site reveals a physical and metabolic interconnection between the endocytic pathway and mitochondria.

INTRODUCTION

Within the endomembrane system, organelles are tightly interconnected via vesicles that carry lipids and proteins between them. Mitochondria, which form a tubular network across the entire cell and have essential functions in respiration, Fe-S cluster generation, amino acid biosynthesis, apoptosis, and carbohydrate metabolism, are largely excluded from this vesicular transport system. Consequently, mitochondria have to rely on alternative mechanisms to exchange proteins, lipids, and metabolites with other organelles. Initially identified via electron microscopy as 10–30 nm junctions, contact sites are now well-accepted, but poorly characterized sites that could mediate non-vesicular exchange between organelles (Elbaz and Schuldiner, 2011). Multiple contact sites have been described between the endoplasmic reticulum (ER) and other organelles, including plasma membrane, Golgi, and endosomes (Hanada, 2010 ; Eden et al., 2010; Giordano et al., 2013; Manford et al., 2012), but also mitochondria, named mitochondrial-associated membranes (MAMs; Achleitner et al., 1999; de Brito and Scorrano, 2008; Elbaz and Schuldiner, 2011; Kornmann et al., 2009). MAMs have been implicated in the transport of Ca^{2+} and phospholipids from the ER to the inner mitochondrial membrane (Osman et al., 2011). In yeast, the ER is attached to the mitochondrial surface via the ER-mitochondria encounter structure (ERMES), which consists of two integral outer mitochondrial membrane proteins, Mdm34 and Mdm10, the ER protein Mmm1, and the peripheral outer mitochondrial membrane protein Mdm12 (Kornmann et al., 2009), although the function of ERMES in lipid transfer has been debated (Nguyen et al., 2012).

Mitochondrial and vacuolar biogenesis seem to affect each other. For instance, vacuole morphology is affected by a loss of the cardiolipin synthase Crd1 (Chen et al., 2008), whereas several endosomal and vacuolar mutants, including all V-ATPase subunits, result in a mitochondrial petite phenotype (Merz and Westermann, 2009) or affect mitochondrial functions in longevity (Hughes and Gottschling, 2012). We considered the possibility that some of the identified connections may be the result of a direct contact between both organelles.

RESULTS

Identification of a Vacuole-Mitochondria Contact Site

To search for membrane contacts, we simultaneously traced mitochondria, labeled with OM45-GFP, and fluorescently stained vacuoles and observed repetitive contacts between both organelles (Figure 1A). Using our newly established electron tomography method, we confirmed such contacts at the ultrastructural level in 200–250 nm cryosections. Vacuole-apposed mitochondria formed contact sites (i.e., distance of two adjacent membranes less than 10 nm; Holthuis and Levine, 2005) approximately 100 nm wide, with crista junctions close by (Figure 1B).

To identify components involved in these contacts, we screened candidate proteins of the vacuole. Because contact sites are rare in wild-type cells, the analysis of deletion mutants proved to be difficult. Because it was postulated that

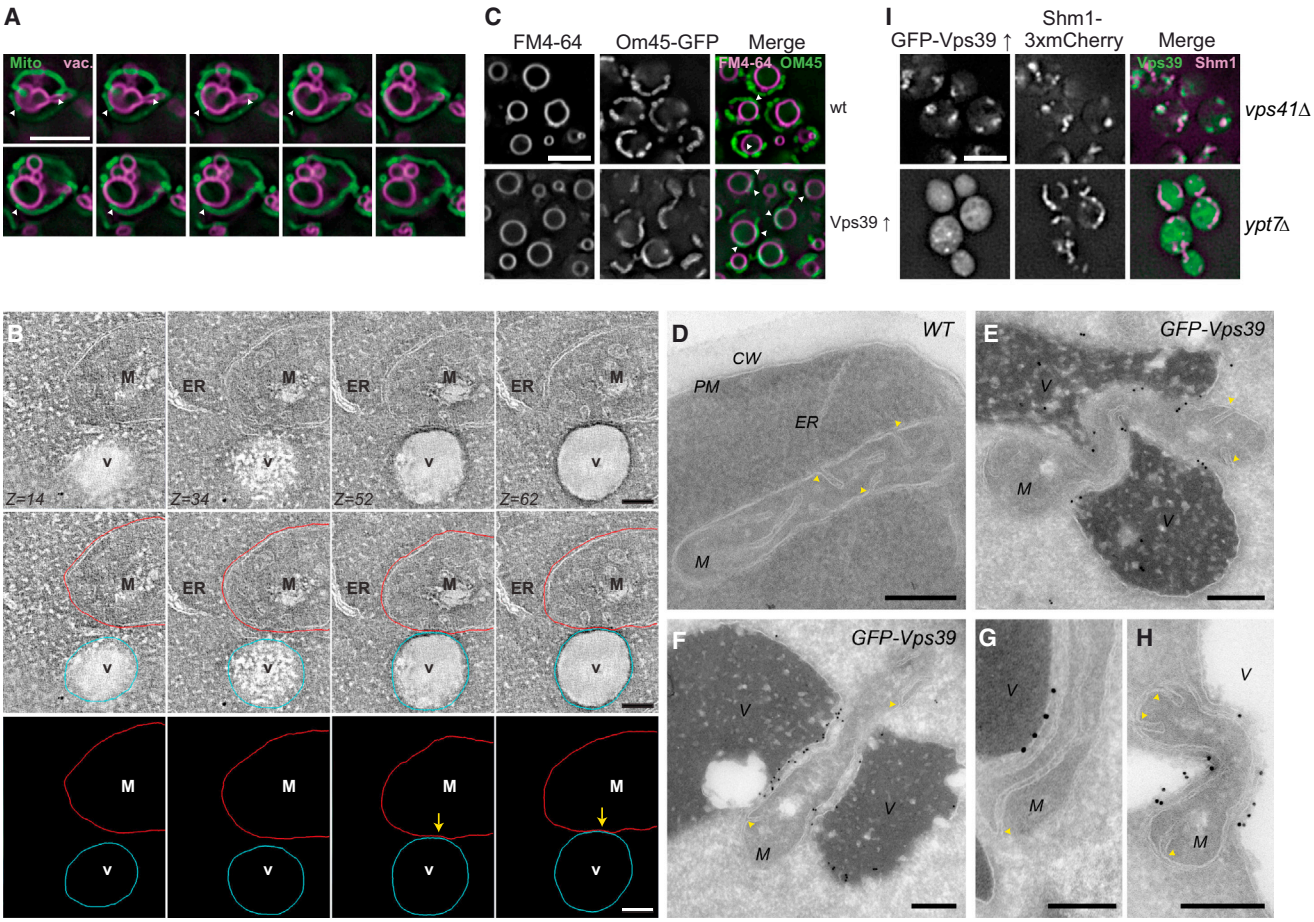

Figure 1. Identification of Vps39-Dependent Contact Sites

(A) Contacts between vacuoles and mitochondria in wild-type. Z stack of consecutive 0.2 μm sections of a wild-type (WT) strain expressing the mitochondrial marker protein Om45-GFP. Vacuoles were stained with FM4-64. Cells were depicted by fluorescence microscopy. Arrowheads indicate contacts; scale bars represent 5 μm in (A), (C), and (I).

(B) Sequential tomograph slices (with or without contours, or contours alone; mitochondrion, red; vacuole, blue) illustrating the contact site between a mitochondrion and a vacuole, which is highlighted with an arrow. Scale bar represents 100 nm.

(C) Vps39-induced vacuole-mitochondria contacts. Localization of mitochondria and vacuoles was analyzed as in (A) in a WT (upper) and a strain overexpressing Vps39 under control of the *TEF1* promoter (lower). Arrowheads indicate vacuole-mitochondria contacts.

(D–H) Ultrastructural analysis of a strain overexpressing GFP-Vps39 (E–H) in comparison to a WT strain (D). The fusion protein was visualized using antibodies against GFP. GFP-Vps39 localizes to vacuoles and is enriched at contact sites between vacuoles and mitochondria. CW, cell wall; PM, plasma membrane; ER, endoplasmic reticulum; M, mitochondria; V, vacuoles. Scale bars represent 200 nm. Yellow arrowheads indicate crista junctions from where cristae protrude into the matrix lumen.

(I) Contacts require Ypt7-associated Vps39, but not its HOPS integration. N-terminally GFP tagged Vps39 was expressed under the *TEF1* promoter in *vps41*Δ or *ypt7*Δ strains. Mitochondria were depicted with Shm1-3xmCherry.

See also Figures S1 and S2.

hyperactivation of a tether should increase the extent of the respective membrane contact site (MCS) (Pan et al., 2000; Helle et al., 2013), we used overexpression to test if contacts between vacuoles and mitochondria would enlarge. During SNARE-dependent membrane fusion, vacuoles are initially tethered to endosomes or other vacuoles via the HOPS tethering complex. Within HOPS, Vps41/Vam2 and Vps39/Vam6 directly bind the Rab GTPase Ypt7 (Balderhaar and Ungermann, 2013; Bröcker et al., 2012). We reasoned that the same machinery might have the potential to also interact with mitochondria. Neither overexpression of Vps41, nor of Vps11, which is critical for HOPS assembly, resulted in any mitochondrial accumulation, and both proteins localized largely to the cytosol or vacuoles (Figures S1A, S1C, S1D, and S1G available online). Likewise, overexpression of Ypt7 resulted in dot-like structures proximal to the vacuole (Figure S1A; Balderhaar et al., 2010), which did not overlap with mitochondria and were identified as multivesicular bodies with immunoelectron microscopy (IEM) (Figures S1E–S1G). Strikingly, overexpression of Vps39 caused a massive expansion of the contacts between vacuoles and mitochondria (Figure 1C). GFP tagging of Vps39 further showed that Vps39 itself accumulated at the contact sites, which extended along the surface of vacuoles (Figure S1A). This strong apposition of both organelles led to a clustered appearance of mitochondria (Figure S1A).

Ultrastructural analyses with IEM revealed a strong Vps39-dependent apposition of mitochondria to vacuoles, and located Vps39 mainly in the contact sites (Figures 1E–1H). Hereafter, we will refer to these contact sites as the vacuole and mitochondria patches (vCLAMPs). Interestingly, an increase of contacts also affected the mitochondrial membrane morphology: cristae were visible almost exclusively outside the contact site and in wild-type (Figures 1D, 1G, 1H, and S1B). At Vps39-enriched contacts, inner membranes appeared flat and aligned along the outer membrane. The number of cristae per micrometer of membrane was strongly reduced (Figures 1E–1H and S1B), suggesting that either vCLAMPs preferentially form at sites were cristae are excluded or that vCLAMP formation itself influences mitochondrial inner membrane organization.

To test whether Vps39 needed to be part of the HOPS complex for contact formation, we monitored Vps39-induced contacts in *vps41*Δ or *vps11*Δ mutants, which do not form an intact HOPS complex anymore (Ostrowicz et al., 2010). Although neither deletion affected mitochondrial morphology per se (Figure S1I), overproduction of Vps39 resulted in massive coclustering of mitochondria and vacuolar fragments (Figures 1I and S1H). In contrast, in the absence of its vacuolar binding partner Ypt7, GFP-Vps39 became cytosolic, and mitochondrial morphology was restored (Figure 1I). We thus concluded that the contacts are Vps39- rather than HOPS-specific and depend on Ypt7.

Crosstalk between Two Mitochondrial Membrane Contact Sites

In a search for contact site function, we initially tested for a role in mitophagy, which requires HOPS. However, extension of vCLAMPs did not affect mitophagy (Figure S2A); their formation was independent of known mitophagy-specific proteins (Figure S2B; Kanki et al., 2009), and did not affect mitochondrial inheritance (Figure S2C). We then analyzed previously identified contact sites at mitochondria and vacuoles relative to vCLAMPs. In agreement with our IEM analyses (Figure 1), we did not observe overlap with the nuclear-vacuolar junction, marked by the ER protein Nvj1 (Pan et al., 2000), endosomes, or peroxisomes labeled with Vps8 and Pts1, respectively (Figure 2A). In contrast, the mitochondrial ERMES subunit Mdm34 was found in almost half of all cases in proximity to vCLAMPs (Figures 2A and S3B), suggesting that ER-mitochondrial contacts and vCLAMPs might influence each other. We therefore wondered if the known growth defects of ERMES mutants (Kornmann et al., 2009) would be influenced by enhanced vacuolar-mitochondrial contacts. Strikingly, Vps39 overproduction, which did not affect growth of wild-type cells, rescued growth of *mdm10* and *mdm12* mutants on glucose medium. In addition, growth on glycerol, where ERMES mutants are inviable, was partially restored, suggesting that residual vCLAMPs formation during respiration is sufficient to compensate for a loss of ERMES-mediated contact sites (Figure 2B). Moreover, strongly enhanced vCLAMPs were observed in both mutants, which is likely due to the condensed shape of mitochondria in ERMES mutants (Figure S3A). Thus, ERMES itself is not needed to generate vCLAMPs, whereas loss of ERMES might enhance vCLAMP formation. These observations suggest that both vacuolar and ER contacts contribute to mitochondrial functionality possibly carrying partially redundant functions.

Metabolic Control of Vacuole-Mitochondrial Contacts

Because mitochondria strongly proliferate during respiratory growth on glycerol, vacuolar and ER contact sites might be affected under these conditions. Indeed, the number of ERMES sites as marked by Mdm34-GFP, Mdm12-GFP, or Mmm1-GFP strongly increased in cells grown in glycerol as the sole carbon source (Figures 2C and 2D), suggesting that ERMES sites (Figure 2E) become more important during respiration. To our surprise, contacts between mitochondria and vacuoles significantly decreased under the same conditions (Figures 3A and 3B). Likewise, the fraction of Vps39 that could be copurified with mitochondria in glucose was lost in mitochondrial fractions if purification was done from glycerol-grown cells (Figure 3C). We then tested if the re-addition of glucose to the medium would establish vCLAMPs. The reappearance did not occur instantaneously and was best seen after 180 min. During this period, a large portion of the mitochondria was degraded by mitophagy as apparent from the vacuolar luminal staining (Figure 3D). This suggests that vCLAMPs could be important in glucose-grown cells and partially compensate for the ERMES-mediated mitochondria-ER contacts. Under respiratory growth conditions, vCLAMPs are however strongly reduced, suggesting a tight metabolic connection between both contact sites.

We next asked for the potential molecular mechanism of regulation, and focused on Vps39 as the most obvious candidate, which binds Ypt7. To ask if the interaction of Vps39 and Ypt7 is regulated by metabolic changes, we relocalized Vps39 by tagging the endogenous protein with a C-terminal Fis1 transmembrane domain to the mitochondrial surface (Figure 3E), which was confirmed by colocalization with a mitochondria-targeted BFP (Figure 3F). Mitochondria containing Vps39-Fis1 remained filamentous with distinct sites where Vps39 was enriched and close contacts with vacuoles were observed with fluorescence microscopy (Figure 3F) and confirmed with ultrastructural analysis (Figures 3G, S4A, and S4B). This contact was not as strong as that observed for overexpressed Vps39, and some mitochondria remained separated from the vacuoles (Figures 3F, 3G, and S4B–S4E). Absence of Ypt7 abolished accumulation of Vps39-Fis1 and led to an even distribution along the mitochondrial filaments as reported for the wild-type Fis1 protein (Mozdy et al., 2000; Figure 3F). This result supports the previous finding that vCLAMPs establishment depends on Ypt7-Vps39 (Figures 1C and 1I). Mitochondria-anchored Vps39-Fis1 appeared to bind other HOPS subunits and promote vacuolar fusion because the vacuoles remained largely round. Importantly, mitochondria-anchored Vps39 remained in dot-like structures associated with the vacuoles even in glycerol (Figure 3F), conditions under which the normal vCLAMPs are strongly reduced. This shows that the Ypt7-Vps39 interaction does not respond to respiratory growth conditions, but only the contact between Vps39 and mitochondria.

Phosphorylation is a common mechanism to regulate protein function in response to growth condition changes. Because the ability of Vps39 appeared to be regulated by cellular metabolic adjustments to carbon sources such as glycerol, we asked whether this HOPS subunit might be a target of phosphorylation. We therefore purified the protein from either glucose or glycerol-grown cells and searched for phosphorylation sites (Figure S3C).

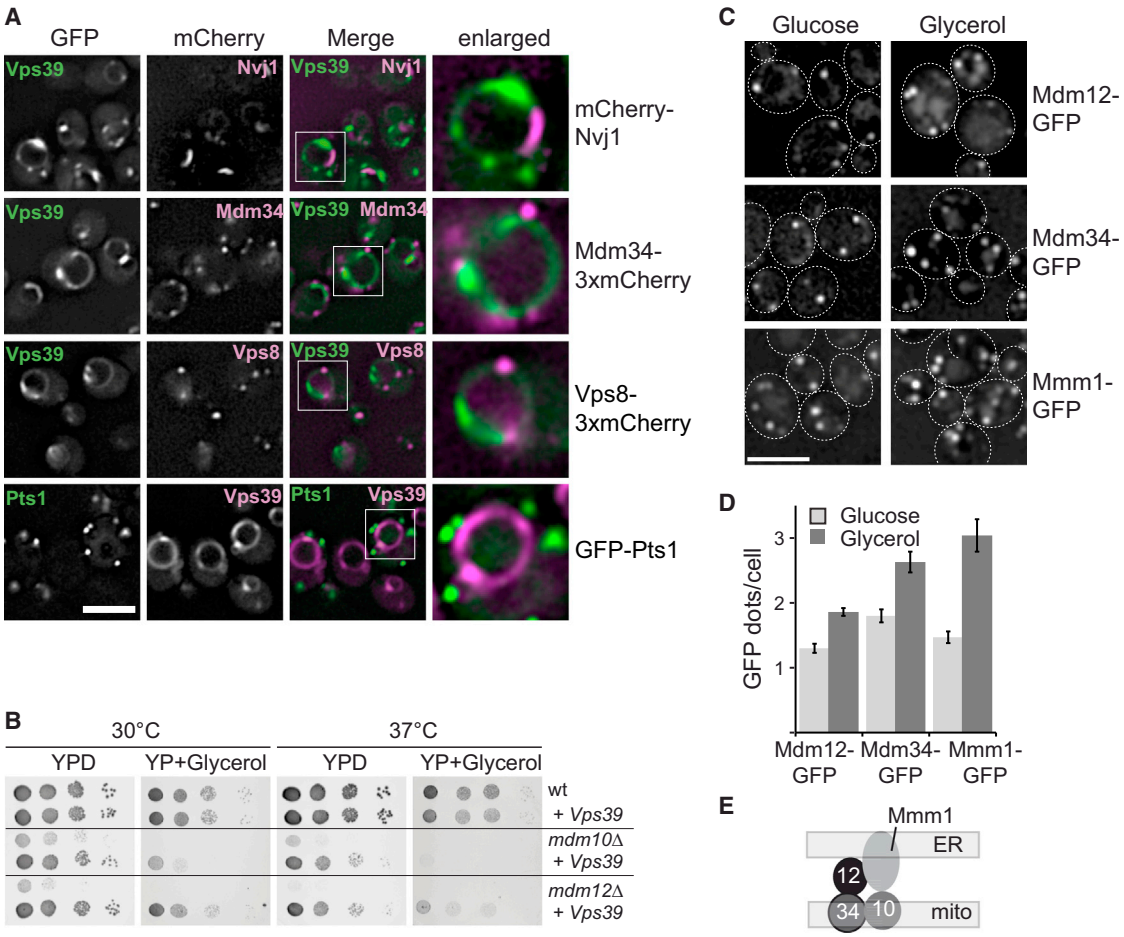

Figure 2. Crosstalk of vCLAMPs with Other Membrane Contact Sites

(A) Relative distribution of Vps39 contacts to membrane contact sites and other organelles. The indicated marker proteins (Nvj1 for the nuclear-vacuolar junctions, Vps8 for endosomes, and Mdm34 for ERMES) were tagged with 3xmCherry. For peroxisomes, GFP-Pts1 was analyzed in the presence of overexpressed mCherry-Vps39. White boxes indicate enlarged areas. Scale bars in (A) and (C) represent 5 μm. Quantification is described in Figure S3B.

(B) Influence of vCLAMPs on ERMES mutants. ERMES mutant strains *mdm12*Δ and *mdm10*Δ with or without overexpressed GFP-Vps39 were spotted in 10-fold dilutions onto plates containing either glucose or glycerol.

(C and D) ERMES proliferates under respiratory growth conditions. C-terminally GFP-tagged ERMES subunits Mdm12, Mdm34, and Mmm1 were depicted in glucose- or glycerol-containing medium. For growth in glycerol, glucose-grown cells were washed twice with water, diluted in glycerol-containing media, and grown for 6 hr before imaging. Sum projections of z stacks of an entire cell are shown. Quantification of 350–400 cells from three independent experiments is shown in (D). Data are mean ± SD.

(E) Schematic model of the ERMES complex.

See also Figure S3.

Only in glycerol-grown cells, we detected phosphopeptides that matched to residues S246, S247, S249, and S250 within the Vps39 N-terminal part. We therefore generated phosphomimetic (S-D) and nonphosphorylatable (S-A) versions of Vps39, in which all identified phosphorylated serines were mutated, and expressed them instead of wild-type Vps39. In agreement with the observed phosphorylation status of Vps39 in glycerol, we detected vCLAMPs in cells expressing Vps39 S-A, whereas cells with Vps39 S-D showed strongly reduced vCLAMPs (Figures 4A and 4B). Importantly, cells expressing Vps39 S-D still maintained round vacuoles, indicating that vacuole biogenesis per se was not affected (Figure 4A). We thus conclude that vCLAMPs are formed and regulated via Vps39 phosphorylation (Figure 4D).

ERMES-mediated ER-mitochondria contact and Vps39-mediated vCLAMPs appeared to be regulated in a reciprocal manner in response to the metabolic status of cells, suggesting that both contacts/structures are involved in similar physiological functions/pathways, but under fundamentally different overall conditions (respiratory versus fermentative metabolism). In agreement with this idea, genetic interaction studies revealed that the combined deletion of *vps39*Δ and *mdm34*Δ was lethal (Figure S3D; Elbaz-Alon et al., 2014 [this issue of *Developmental Cell*]). The absence of Vps39 causes multiple defects that are associated with vesicular transport and vacuolar functionality (Nakamura et al., 1997; Price et al., 2000a, 2000b), which hampers the conclusion that the synthetic lethality is a direct consequence of impaired vCLAMP formation. Hence, we asked whether the

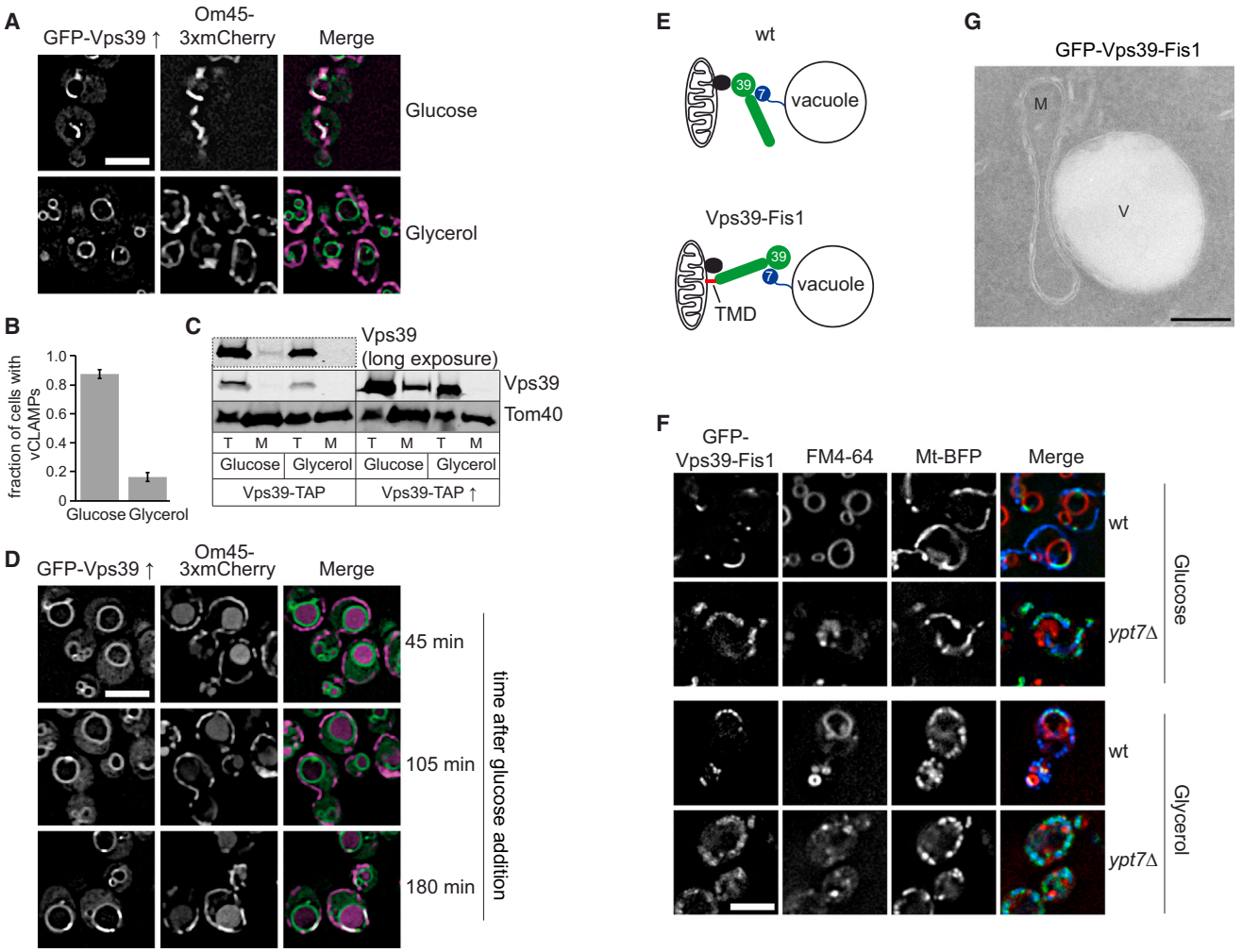

Figure 3. vCLAMPs Respond to Respiratory Growth Conditions

(A) Loss of vCLAMPs in respiratory growth conditions. Localization of vacuoles marked by overexpressed GFP-Vps39 and mitochondria labeled with Om45-3xmCherry was monitored with fluorescence microscopy. Cells were grown in medium containing glycerol or glucose as described in the Experimental Procedures. Scale bar represents 5 μm.

(B) Quantification of cells containing vCLAMPs (n = 700) from four independent experiments. Data are mean ± SD.

(C) Association of Vps39 with purified mitochondria is lost in glycerol. Mitochondria were isolated from strains expressing C-terminally TAP-tagged Vps39 under either endogenous promoter or overexpressed from the *GPD1* promoter, which were grown in either glucose- or glycerol-containing medium. Blots were decorated with antibodies against the mitochondrial Tom40 and Vps39. T, total cellular protein; M, purified mitochondria. Dashed box in the top row shows a higher exposure of endogenous Vps39.

(D) Reformation of vCLAMPs occurs after glucose addition. Glucose was added to a final concentration of 2% (w/v) to a glycerol-grown culture as shown in (A) and localization of GFP-Vps39 was followed by fluorescent microscopy at the indicated time points. Scale bar represents 5 μm.

(E) Schematic model of Vps39 topology and its interaction with Ypt7 and with a putative mitochondrial binding partner (black). To the right, the artificial targeting of Vps39 via the mitochondrial Fis1 transmembrane domain (TMD) is shown.

(F) Metabolic control of the Vps39-Ypt7 interaction. N-terminally GFP-tagged Vps39 with a C-terminal Fis1 transmembrane domain was monitored with fluorescence microscopy in WT and *ypt7*Δ cells grown in presence of glucose or glycerol as in (A). Vacuoles were labeled with FM4-64, mitochondria were followed by expression of matrix-targeted BFP. Scale bar represents 5 μm.

(G) Ultrastructural analysis of a strain expressing GFP-Vps39-Fis1 shown in (F). M, mitochondria; V, vacuole. Scale bar represents 200 nm.

See also Figure S4.

Vps39 S-A and S-D variants would affect viability when expressed in the *mdm34*Δ strain because phosphorylation solely regulates vCLAMPs formation and leaves HOPS function unaffected (Figure 4A). Indeed, Vps39 S-A rescued the growth defect caused by the *mdm34*Δ deletion partially, whereas Vps39 S-D did not rescue, but decreased cellular fitness even greater (Figures 4C and S3D). However, unlike the *vps39* deletion, the Vps39 S-D mutant was not synthetically lethal with *mdm34*Δ. Because the mutated versions of Vps39 were expressed under control of the endogenous *VPS39* promoter, this result also shows that phosphorylation of Vps39 controls vCLAMP function independently from overexpression.

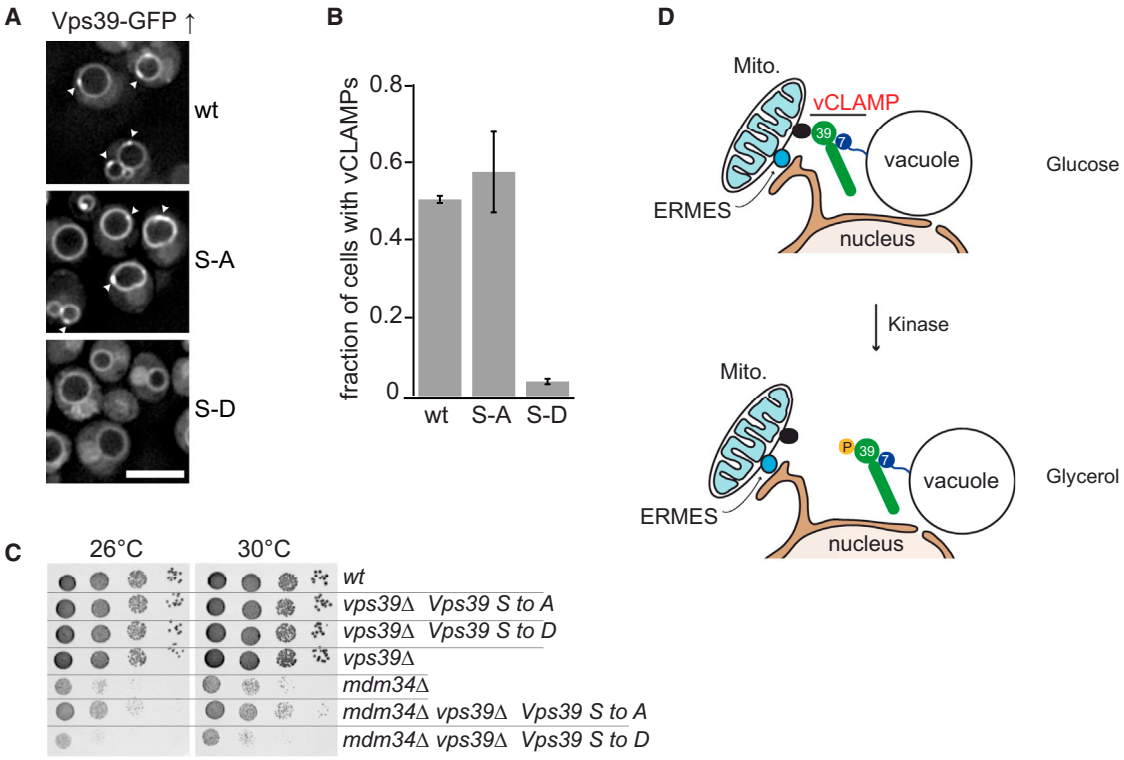

Figure 4. Phosphorylation of Vps39 Affects vCLAMP Formation

(A and B) Mutants in Vps39 reproduce the metabolic dynamics of vCLAMPs. Serines at positions 246, 247, 249, and 250 in Vps39 were mutated into alanine or aspartate residues, and the localization of the corresponding GFP-tagged WT, S-A, and S-D variants expressed under control of the *TEFpr* in *vps39*Δ cells was monitored with fluorescence microscopy. Arrowheads indicate sites of GFP-Vps39 accumulation. Quantification of 400 cells in total from three independent experiments is shown in (B). Data are mean ± SD.

(C) Strain deleted for *MDM34* was mated with a *vps39*Δ strain expressing Vps39 WT, S-A, or S-D from an integrative plasmid under control of the endogenous *VPS39pr*. Diploids were sporulated and tetrads were dissected (Figure S3D). Obtained mutant strains were spotted in sequential 1:10 dilutions on YPD medium and incubated at different temperatures.

(D) Model of vCLAMPs dynamics relative to other intracellular membrane contact sites. Contacts are lost upon phosphorylation of Vps39. ERMES, ER-mitochondria encounter structure.

See also Figure S3.

DISCUSSION

We demonstrate here the identification of a direct physical contact between mitochondria and vacuoles. Contact sites are formed by Vps39 and Ypt7, but independently of HOPS, suggesting that Vps39 has a dual role on vacuoles. The nucleus-vacuole junctions in yeast and ER-late endosome contact sites in metazoans are formed by Vac8 and Rab7, respectively, two factors involved in vesicular transport processes in the endolysosomal system (Pan et al., 2000; Rocha et al., 2009). A participation of fusion regulators in membrane contact site formation might allow coregulation of vesicular and nonvesicular transport routes to integrate both types of pathways and make intracellular transport process more efficient (Hönscher and Ungermann, 2014). Furthermore, vCLAMPs are regulated by phosphorylation of Vps39, indicating that they are dynamic metabolic hubs intimately embedded into cellular physiology. Known metabolically regulated kinases include the TOR kinases, Snf1/AMPK and protein kinase A (De Virgilio, 2012; Jewell et al., 2013). Interestingly, our bioinformatic analyses indicate the presence of a Snf1 consensus site within Vps39. The function of vCLAMPs as a metabolic hub is supported by the physical proximity and genetic interaction with ERMES components and the effects of vCLAMP propagation on the organization of the inner mitochondrial membrane. Several studies previously showed that mutants in the endocytic pathway have strong effects on mitochondrial biogenesis. A genome-wide screen identified Vps39 among the many genes that result in mitochondrial petite phenotypes (Merz and Westermann, 2009). In turn, mutants in cardiolipin synthase or phosphatidylglycerolphosphate synthase, two proteins involved in the generation of cardiolipin, a mitochondria-specific lipid, affect vacuole morphology (Chen et al., 2008), although not fusion (Stroupe, 2012). This suggests that both organelles indeed exchange lipids and other nutrients. In agreement, double mutants of *vps39* and ERMES are synthetically lethal, and recovered mitochondria from cells depleted for both partners have strongly altered phospholipid profiles (Elbaz-Alon et al., 2014). This suggests that vCLAMPs could be an alternative site for the transfer of phospholipids (and/or other metabolites) in addition to the ERMES complex, which could explain the discrepancies in the results on lipid transfer of ERMES mutants (Kornmann et al., 2009, 2011; Nguyen et al.,

2012; Elbaz-Alon et al., 2014). Furthermore, both Mdm10 and Mdm12 are critical for the biogenesis of essential mitochondrial outer membrane proteins (Wiedemann et al., 2009), suggesting that ERMES mutants may have additional defects that cannot be compensated by vCLAMPs. Yeast favors ERMES in glycerol conditions while the abundance vCLAMPs decreases (Figures 2C, 2D, 3A, and 3B), suggesting that both sites are regulated in a reciprocal manner and gain importance under different physiological conditions. In agreement with this, Elbaz-Alon and colleagues reported that absence of Vps39 increases abundance of ERMES foci (Elbaz-Alon et al., 2014). Interestingly, upregulation of Vps39 did not decrease the number of ERMES foci (not shown), indicating that the reciprocal regulation is not mediated merely by the physical presence of the other MCSs, but due to the physiological requirement of an alternative route. Because vacuoles are closely linked to amino acid sensing via the lysosomal EGO/LamTOR and TORC1 (Jewell et al., 2013), and amino acid catabolism funnels the carbon backbone into the citric acid cycle, additional connections beyond lipid transfer are likely important. These might be critical to integrate the metabolic and nutritional status of the cell into different transport pathways. Recently, Daniele and colleagues reported a physical contact between mitochondria and melanosomes, lysosome-related organelles in pigment cells, revealing that contact sites between mitochondria and organelles of the endolysosomal system probably exist in higher eukaryotes as well (Daniele et al., 2014). We expect that further analysis of vCLAMPs will provide detailed insights into the organellar crosstalk via MCSs.

EXPERIMENTAL PROCEDURES

Yeast Strains, Plasmids, and Molecular Biology

Strains, plasmids, and primers used and description of site directed mutagenesis of *VPS39* are presented in the Supplemental Experimental Procedures. Terminal tagging and deletion of genes were done using homologous recombination of PCR fragments (Janke et al., 2004).

Fluorescence Microscopy

Yeast cells were grown to midlog phase in yeast extract peptone dextrose (YPD), yeast extract peptone glycerol, or synthetic complete medium lacking selected amino acids or nucleotides, collected by centrifugation, washed once with synthetic complete medium supplemented with all amino acids and the respective carbon source, and immediately analyzed with fluorescence microscopy. For FM4-64 staining of vacuoles, cells were incubated with 30 μM FM4-64 for 30 min, washed twice with full medium supplemented with the respective carbon source, and incubated in the same medium without dye for 1 hr. Images were acquired on a Deltavision Elite imaging system (GE Healthcare) or a DM5500 B microscope (Leica). Detailed information about the microscopes and software is provided in the Supplemental Experimental Procedures.

Electron Microscopy and Tomography

Immunoelectron microscopy examinations were performed using a goat anti-GFP antibody (Rockland Immunochemicals) as previously described (Griffith et al., 2008).

The relative distribution of the immunogold labeling in cells overexpressing GFP-Vps39, GFP-Vps41, and GFP-Ypt7 was determined by randomly analyzing 1,000 gold particles per strain. A gold particle was assigned to a well-defined organelle (vCLAMP, vacuole or MVBs) when no further than 15 nm away from the limiting membrane or cytoplasm.

The number of cristae per micrometer was calculated as previously described (Rabouille, 1999). Briefly, in the wild-type strain, 50 mitochondria were randomly selected before to measure their surface section using the point-hit method and to count the number of cristae distinctively forming from the inner membrane of this organelle. In cells overexpressing GFP-Vps39, 50 mitochondria tethered with the vacuole were selected and subsequently the surface section of both the vCLAMP and the unassociated mitochondria surface were measured with the point-hit method. The cristae in these two regions were also counted. The number of cristae per micrometer was obtained by dividing the number of cristae by the length of the surface section.

Electron tomography reconstructions were carried out on 200–250 nm thick cryosections prepared as described elsewhere (M.M., W.G., and F.R., unpublished data). Dual axis tilt series were recorded using a Tecnai 20 electron microscope (FEI) with an angular range of −60 to +60 degrees with 1-degree increments. In this way, each tilt series contained 121 images. The tilt series were aligned using fiducial gold particles and single-axis tilt tomograms were created by combining the two R-weighted back projections using the IMOD program package (Kremer et al., 1996). The tomograms had a final resolution of approximately 4 nm and were mounted into movies using QuickTime software (Apple).

Tetrad Analysis

Two yeast strains with different mating types were streaked out on a double-selective plate to allow mating and diploid cell selection. Diploid cells were cultured in YPD overnight to a stationary phase, pelleted, resuspended in residual medium, and plated as one large drop onto potassium acetate plates (1% [w/v] potassium acetate, 3% [w/v] agar). After 3 days, a small amount of cells was dissolved in 200 μl sterile water supplemented with 5 U/ml zymolyase (MP Biomedicals) and incubated for 10 min at room temperature. The reaction was stopped by a short incubation on ice and the addition of 400 μl sterile water. Then 15 μl of this mixture were streaked onto a YPD plate, and tetrads were separated with the help of a micromanipulator and grown for at least 3 days. The genotype of the spores was determined by testing growth on different selective media.

Serial Drop Dilution Assays

Cells were grown in YPD to logarithmic phase, washed twice with sterile water, and diluted to an optical density 600 (OD_{600}) of 0.25. Serial dilutions (1:10) were spotted onto different plates and imaged after growth for 2–4 days at different temperatures.

Purification of Mitochondria

Yeast cells were grown in full medium containing either glucose or glycerol as a carbon source. The main culture was inoculated from a preculture grown for either 12 hr (glucose) or 26 hr (glycerol) with an appropriate amount to reach 2.5 OD_{600} after 12 hr of growth, then 2,500 OD_{600} units of cells were harvested and incubated in dithiothreitol (DTT) buffer (0.1 M Tris-H_2SO_4, pH 9.4, 10 mM DTT) for 20 min at 30°C. Pellets were resuspended in spheroplasting buffer (1.2 M sorbitol, 20 mM potassium phosphate, pH 7.4) and treated with zymolyase (MP Biomedicals) for 20 min at 30°C. Spheroplasts were homogenized in buffer (0.6 M sorbitol, 10 mM Tris-HCl, pH 7.4, 1 mM EDTA, 1 mM phenylmethanesulfonylfluoride, 0.2% [w/v] BSA [essentially fatty acid-free, Sigma-Aldrich]) with 15 strokes using a tight-fitting potter. After two subsequent centrifugation steps for 5 min at 1,500 × *g* and 4000 × *g*, the final supernatant was centrifuged at 12,000 × *g* for 15 min to pellet mitochondria. Crude mitochondrial fractions were resuspended in SEM buffer (250 mM sucrose, 1 mM EDTA, 10 mM MOPS-KOH, pH 7.2) and diluted to a protein concentration of 5 mg/ml. One milliliter of the fraction was loaded on top of a 60%, 32%, 23%, and 15% (w/v) step sucrose gradient in EM buffer (1 mM EDTA, 10 mM MOPS-KOH, pH 7.2) and centrifuged for 1 hr at 134,000 × *g* at 4°C. Pure mitochondria were collected at the 60%/32% sucrose interface, diluted with two volumes of SEM buffer, and centrifuged at 10,000 × *g* for 5 min. Pellets were resuspended in SEM buffer and protein concentration was estimated. Twenty-microgram aliquots of total mitochondrial protein were centrifuged and pellets were resuspended in 2× SDS sample buffer (60 mM Tris, pH 6.8, 2% SDS, 10% glycerol, 5% 2-mercaptoethanol, and 0.005% [w/v] bromophenol blue) and boiled for 5 min.

Purification of Vps39 from Yeast Cells and Protein Mass Spectrometry

Vps39 was purified via a C-terminal TAP-tag from cells grown in either glucose or glycerol. See the Supplemental Experimental Procedures for more details.

Preparation of Total Protein Extract

One OD_{600} unit of cells was collected and resuspended in 0.5 ml of 10% (w/v) trichloroacetic acid and incubated for 30 min at 4°C. Precipitated proteins were washed once in ice-cold acetone, air-dried, resuspended in 1× SDS sample buffer and boiled for 5 min.

SUPPLEMENTAL INFORMATION

Supplemental Information includes Supplemental Experimental Procedures and four figures and can be found with this article online at http://dx.doi.org/10.1016/j.devcel.2014.06.006.

ACKNOWLEDGMENTS

We thank our colleagues Karin Busch, Benoît Kornmann, Ralf Erdmann, Walter Neupert, Thomas Langer, Tim Levine, Roland Lill, Klaus Pfanner, Andreas Reichert, Janet Shaw, and Benedikt Westermann for suggestions, support, discussion, and feedback and Henning Kleine Balderhaar and Clemens Ostrowicz for contributions during initial phases of the project. This work was supported by a grant of the State of Lower Saxony, Hannover, Germany (ZN2444), the SFB 944 (project P11), and by the Hans-Mühlenhoff foundation (to C.U.). F.R. is supported by ECHO (700.59.003), ALW Open Program (821.02.017 and 822.02.014), DFG-NWO cooperation (DN82-303), and ZonMW VICI (016.130.606) grants. M.v.d.L. is supported by the Deutsche Forschungsgemeinschaft, SFB 746, and the Excellence initiative of the German Federal and State Governments (EXC 294 BIOSS).

Received: October 14, 2013
Revised: April 4, 2014
Accepted: June 9, 2014
Published: July 14, 2014

REFERENCES

Achleitner, G., Gaigg, B., Krasser, A., Kainersdorfer, E., Kohlwein, S.D., Perktold, A., Zellnig, G., and Daum, G. (1999). Association between the endoplasmic reticulum and mitochondria of yeast facilitates interorganelle transport of phospholipids through membrane contact. Eur. J. Biochem. *264*, 545–553.

Balderhaar, H.J.K., and Ungermann, C. (2013). CORVET and HOPS tethering complexes - coordinators of endosome and lysosome fusion. J. Cell Sci. *126*, 1307–1316.

Balderhaar, H.J.K., Arlt, H., Ostrowicz, C., Bröcker, C., Sündermann, F., Brandt, R., Babst, M., and Ungermann, C. (2010). The Rab GTPase Ypt7 is linked to retromer-mediated receptor recycling and fusion at the yeast late endosome. J. Cell Sci. *123*, 4085–4094.

Bröcker, C., Kuhlee, A., Gatsogiannis, C., Balderhaar, H.J.K., Hönscher, C., Engelbrecht-Vandré, S., Ungermann, C., and Raunser, S. (2012). Molecular architecture of the multisubunit homotypic fusion and vacuole protein sorting (HOPS) tethering complex. Proc. Natl. Acad. Sci. USA *109*, 1991–1996.

Chen, S., Tarsio, M., Kane, P.M., and Greenberg, M.L. (2008). Cardiolipin mediates cross-talk between mitochondria and the vacuole. Mol. Biol. Cell *19*, 5047–5058.

Daniele, T., Hurbain, I., Vago, R., Casari, G., Raposo, G., Tacchetti, C., and Schiaffino, M.V. (2014). Mitochondria and melanosomes establish physical contacts modulated by Mfn2 and involved in organelle biogenesis. Curr. Biol. *24*, 393–403.

de Brito, O.M., and Scorrano, L. (2008). Mitofusin 2 tethers endoplasmic reticulum to mitochondria. Nature *456*, 605–610.

De Virgilio, C. (2012). The essence of yeast quiescence. FEMS Microbiol. Rev. *36*, 306–339.

Eden, E.R., White, I.J., Tsapara, A., and Futter, C.E. (2010). Membrane contacts between endosomes and ER provide sites for PTP1B-epidermal growth factor receptor interaction. Nat. Cell Biol. *12*, 267–272.

Elbaz, Y., and Schuldiner, M. (2011). Staying in touch: the molecular era of organelle contact sites. Trends Biochem. Sci. *36*, 616–623.

Elbaz-Alon, Y., Rosenfeld-Gur, E., Shinder, V., Futerman, A.H., Geiger, T., and Schuldiner, M. (2014). A dynamic interface between vacuoles and mitochondria in yeast. Dev. Cell *30*, this issue, 95–102.

Giordano, F., Saheki, Y., Idevall-Hagren, O., Colombo, S.F., Pirruccello, M., Milosevic, I., Gracheva, E.O., Bagriantsev, S.N., Borgese, N., and De Camilli, P. (2013). PI(4,5)P(2)-dependent and Ca(2+)-regulated ER-PM interactions mediated by the extended synaptotagmins. Cell *153*, 1494–1509.

Griffith, J., Mari, M., De Mazière, A., and Reggiori, F. (2008). A cryosectioning procedure for the ultrastructural analysis and the immunogold labelling of yeast Saccharomyces cerevisiae. Traffic *9*, 1060–1072.

Hanada, K. (2010). Intracellular trafficking of ceramide by ceramide transfer protein. Proc. Jpn. Acad., Ser. B, Phys. Biol. Sci. *86*, 426–437.

Helle, S.C., Kanfer, G., Kolar, K., Lang, A., Michel, A.H., and Kornmann, B. (2013). Organization and function of membrane contact sites. Biochim Biophys Acta. *1833*, 2526–2541.

Holthuis, J.C.M., and Levine, T.P. (2005). Lipid traffic: floppy drives and a superhighway. Nat. Rev. Mol. Cell Biol. *6*, 209–220.

Hönscher, C., and Ungermann, C. (2014). A close-up view of membrane contact sites between the endoplasmic reticulum and the endolysosomal system: From yeast to man. Crit. Rev. Biochem. Mol. Biol. *49*, 262–268.

Hughes, A.L., and Gottschling, D.E. (2012). An early age increase in vacuolar pH limits mitochondrial function and lifespan in yeast. Nature *492*, 261–265.

Janke, C., Magiera, M.M., Rathfelder, N., Taxis, C., Reber, S., Maekawa, H., Moreno-Borchart, A., Doenges, G., Schwob, E., Schiebel, E., and Knop, M. (2004). A versatile toolbox for PCR-based tagging of yeast genes: new fluorescent proteins, more markers and promoter substitution cassettes. Yeast *21*, 947–962.

Jewell, J.L., Russell, R.C., and Guan, K.-L. (2013). Amino acid signalling upstream of mTOR. Nat. Rev. Mol. Cell Biol. *14*, 133–139.

Kanki, T., Wang, K., Cao, Y., Baba, M., and Klionsky, D.J. (2009). Atg32 is a mitochondrial protein that confers selectivity during mitophagy. Dev. Cell *17*, 98–109.

Kornmann, B., Currie, E., Collins, S.R., Schuldiner, M., Nunnari, J., Weissman, J.S., and Walter, P. (2009). An ER-mitochondria tethering complex revealed by a synthetic biology screen. Science *325*, 477–481.

Kornmann, B., Osman, C., and Walter, P. (2011). The conserved GTPase Gem1 regulates endoplasmic reticulum-mitochondria connections. Proc. Natl. Acad. Sci. USA *108*, 14151–14156.

Kremer, J.R., Mastronarde, D.N., and Mcintosh, J.R. (1996). Computer visualization of three-dimensional image data using IMOD. J. Struct. Biol. *116*, 71–76.

Manford, A.G., Stefan, C.J., Yuan, H.L., Macgurn, J.A., and Emr, S.D. (2012). ER-to-plasma membrane tethering proteins regulate cell signaling and ER morphology. Dev. Cell *23*, 1129–1140.

Merz, S., and Westermann, B. (2009). Genome-wide deletion mutant analysis reveals genes required for respiratory growth, mitochondrial genome maintenance and mitochondrial protein synthesis in Saccharomyces cerevisiae. Genome Biol. *10*, R95.

Mozdy, A.D., McCaffery, J.M., and Shaw, J.M. (2000). Dnm1p GTPase-mediated mitochondrial fission is a multi-step process requiring the novel integral membrane component Fis1p. J. Cell Biol. *151*, 367–380.

Nakamura, N., Hirata, A., Ohsumi, Y., and Wada, Y. (1997). Vam2/Vps41p and Vam6/Vps39p are components of a protein complex on the vacuolar membranes and involved in the vacuolar assembly in the yeast Saccharomyces cerevisiae. J. Biol. Chem. *272*, 11344–11349.

Nguyen, T.T., Lewandowska, A., Choi, J.-Y., Markgraf, D.F., Junker, M., Bilgin, M., Ejsing, C.S., Voelker, D.R., Rapoport, T.A., and Shaw, J.M. (2012). Gem1 and ERMES do not directly affect phosphatidylserine transport from ER to mitochondria or mitochondrial inheritance. Traffic *13*, 880–890.

Osman, C., Voelker, D.R., and Langer, T. (2011). Making heads or tails of phospholipids in mitochondria. J. Cell Biol. *192*, 7–16.

Ostrowicz, C.W., Bröcker, C., Ahnert, F., Nordmann, M., Lachmann, J., Peplowska, K., Perz, A., Auffarth, K., Engelbrecht-Vandré, S., and Ungermann, C. (2010). Defined subunit arrangement and rab interactions are

required for functionality of the HOPS tethering complex. Traffic *11*, 1334–1346.

Pan, X., Roberts, P., Chen, Y., Kvam, E., Shulga, N., Huang, K., Lemmon, S., and Goldfarb, D.S. (2000). Nucleus-vacuole junctions in Saccharomyces cerevisiae are formed through the direct interaction of Vac8p with Nvj1p. Mol. Biol. Cell *11*, 2445–2457.

Price, A., Seals, D., Wickner, W., and Ungermann, C. (2000a). The docking stage of yeast vacuole fusion requires the transfer of proteins from a cis-SNARE complex to a Rab/Ypt protein. J. Cell Biol. *148*, 1231–1238.

Price, A., Wickner, W., and Ungermann, C. (2000b). Proteins needed for vesicle budding from the Golgi complex are also required for the docking step of homotypic vacuole fusion. J. Cell Biol. *148*, 1223–1229.

Rabouille, C. (1999). Quantitative aspects of immunogold labeling in embedded and nonembedded sections. Methods Mol. Biol. *117*, 125–144.

Rocha, N., Kuijl, C., van der Kant, R., Janssen, L., Houben, D., Janssen, H., Zwart, W., and Neefjes, J. (2009). Cholesterol sensor ORP1L contacts the ER protein VAP to control Rab7-RILP-p150 Glued and late endosome positioning. J. Cell Biol. *185*, 1209–1225.

Stroupe, C. (2012). The yeast vacuolar Rab GTPase Ypt7p has an activity beyond membrane recruitment of the homotypic fusion and protein sorting-Class C Vps complex. Biochem. J. *443*, 205–211.

Wiedemann, N., Meisinger, C., and Pfanner, N. (2009). Cell biology. Connecting organelles. Science *325*, 403–404.